Radiology Case Reports 16 (2021) 3868–3874

Available online at www.sciencedirect.com

ScienceDirect

journal homepage: www.elsevier.com/locate/radcr

Case report

Metastatic choriocarcinoma with hemorrhagic complications and spontaneous ovarian hyperstimulation syndrome: A case report ☆

Davide Raffaele De Lucia, MD, Anna Castaldo, MD, Valerio D'Agostino, MD, Raffaele Ascione, MD, Ilaria Pesce, MD, Luigi Coppola, MD, Antonio Catelli, MD, Leonardo Radice, MD*

Department of Advanced Biomedical Sciences, University of Naples "Federico II", Via Pansini, 5, Naples 80131, Italy

ARTICLE INFO

Article history:
Received 24 August 2021
Revised 10 September 2021
Accepted 15 September 2021

Keywords:
Gestational choriocarcinoma
Ovarian hyperstimulation syndrome
Choriocarcinoma syndrome
Hypervascular metastases
Hemorrhagic metastases

ABSTRACT

Gestational choriocarcinoma is a malignant trophoblastic tumor arising from any gestational event, even with a long latency period, generally in the reproductive female. It is associated with a high level of beta-human chorionic gonadotropin. Its primary site is usually the uterus but not all patients have a detectable lesion in this site. Regression of the primary tumor after it has metastasized is not uncommon, and one-third of cases manifest as complications of metastatic disease. In this report we present an uncommon case of gestational choriocarcinoma with lung, liver and jejunal metastases at the time of diagnosis without evidence of pelvic disease, in 34-year-old woman. The main points of interest of our case were the development of the ovarian hyperstimulation syndrome with massive multicystic ovarian enlargement induced by high level of beta-human chorionic gonadotropin and the bleeding of jejunal and liver metastases, due to the high vascularity of the tumor tissue, a condition known as "Choriocarcinoma Syndrome". We will focus on the radiological findings of metastases, bleeding complications and ovarian hyperstimulation syndrome.

Introduction

Choriocarcinoma is a rare and highly aggressive neoplasia with trophoblastic differentiation. Two distinct entities are recognized: gestational and non-gestational choriocarcinoma, both associated with high circulating levels of beta-human chorionic gonadotropin (b-hCG) secreted by neoplastic cells.

Non gestational choriocarcinoma is not associated with a previous history of pregnancy and often occurs in children and

Abbreviations: b-hCG, Beta Human Chorionic Gonadotropin; OHSS, Ovarian Hyperstimulation Syndrome; CE-CT, Contrast Enhancement Computed Tomography; HU, Hounsfield Unit; US, Ultrasonography; MRI, Magnetic Resonance Imaging; MIP, Maximum Intensity Projection; MPR, Multiplanar Reconstruction; FSH, Follicle Stimulating Hormone; LH, Luteinizing Hormone; TSH, Thyroid Stimulating Hormone.

☆ Competing Interests: The authors have no conflicts of interest.

* Corresponding author. D.R. De Lucia.
E-mail address: dav.delucia@gmail.com (D.R. De Lucia).

https://doi.org/10.1016/j.radcr.2021.09.031

young adults, arising from midline structure during embryogenesis or primordial germ cell in gonads after birth, characterized by a rapid course with poor prognosis [1].

Gestational choriocarcinoma is associated with gestation and can be placed within the spectrum of gestational trophoblastic neoplasia, being its most aggressive expression. About 25% of gestational forms develop from malignant degeneration of molar pregnancy, 50% can follow full-term pregnancy and the remainder after other gestational events [2]. It may occur months or many years after a previous pregnancy, typically in childbearing age [3]. Gestational choriocarcinoma has a better prognosis than the non-gestational form, given the good results of chemotherapy. It usually originates from the uterus, sometimes without a clearly detectable lesion. Regression of the primary tumor after it has metastasized is not uncommon and one-third of cases manifest with complications of metastatic disease [4–6].

Primary choriocarcinomas are described in other organs such as stomach, lung, pancreas and small intestine [7–9]. Herein we describe a case of metastatic gestational choriocarcinoma without evidence of uterine mass, with jejunal, pulmonary and hepatic diffusion at the moment of diagnosis in a 34-years-old woman. The neoplasm induced in our patient ovarian hyperstimulation syndrome (OHSS), triggered by the high levels of b-hCG and choriocarcinoma syndrome due to bleeding of tumor-induced Jejunal angiodysplasia and hypervascular liver metastases. We will emphasize the radiological findings of metastases, bleeding complications and OHSS.

Case presentation

A 34-year-old woman presented to the emergency department with intense fatigue and a history of amenorrhea for the last 3 months. Her medical history was unremarkable. She had her last pregnancy 3 years earlier. No vaginal bleeding and melena were reported. Laboratory investigations revealed severe anemia (hemoglobin of 4,7 g/dl) and elevated b-hCG level (400,000 IU/ml). The fecal occult blood test was positive. Pelvic ultrasound, initially performed to rule out normal or ectopic pregnancy, revealed a regular size and normal echostructure of uterus and no adnexal mass. Contrast-enhanced Computed Tomography (CE-CT) was required in emergency to look for a bleeding site. Absence of pelvic pathology was confirmed. CT detected multiple hypervascular lesions in both hepatic lobes with hemangioma-like appearance: they showed prevalent peripheral vascularity and central vascular spaces (Fig. 1). Several diffuse pulmonary nodules with soft tissue attenuation were present. The predominant lung lesion was localized to the middle lobe (about 3 cm in size) and appeared mostly hypodense with numerous contextual dilated vessels (Fig. 2). Moreover, we observed a poorly defined jejunal lesion appearing as inhomogeneous mural enhancement with coexistence of intramural swollen vessels. Congestion and early impregnation of mesenteric drainage veins were associated. (Fig. 3). There were no clear signs of jejunal active bleeding foci. No brain lesions were evident. Therefore, a metastatic choriocarcinoma was hypothesized on the basis of CT findings and the very high level of b-hCG. After inconclusive upper and lower gastrointestinal endoscopies, Technetium 99m-labeled red blood cell scintigraphy was performed, making clear that intestinal lesions were the cause of the bleeding. Thus, the patient was transfused and then underwent emergency laparotomy with segmental resection of jejunum (about 37 cm). Histopathologic results confirmed a choriocarcinoma. Macroscopic examination of the intestinal sample showed 2 sessile formations with hemorrhagic aspects involving the intestinal wall up to the muscular layer. Microscopic examination showed anaplastic cytotrophoblasts and syncytiotrophoblasts, absence of chorionic villi, necrosis and hemorrhage. The tumor was strongly positive for b-hCG on immunohistochemistry. After surgery, b-hCG level dropped to 350 IU / mL and hemoglobin remained around 10 mg / dL.

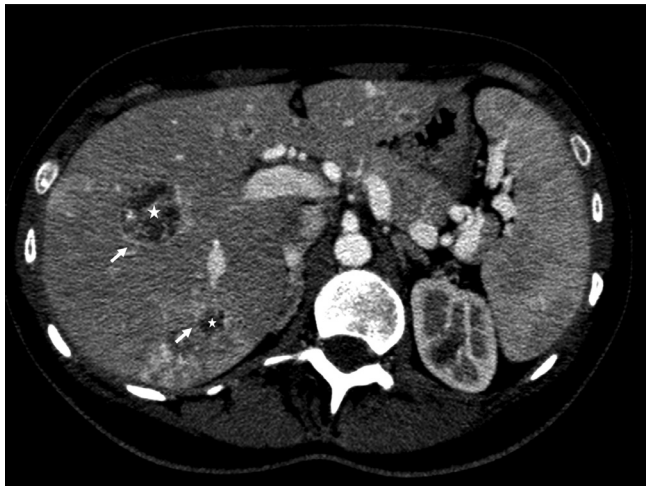

Fig. 1 – Hepatic hemangioma-like metastasis. Axial contrast-enhanced CT image, venous-phase, shows multiple hypervascular lesions in both hepatic lobes with hemangioma-like appearance with peripheral vascularity (arrow) and central vascular spaces (star).

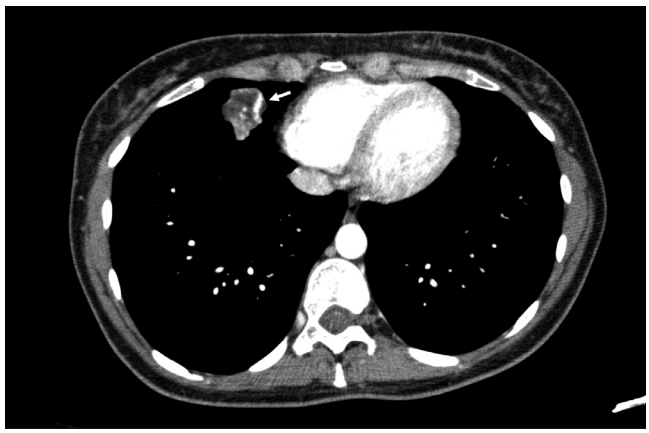

Fig. 2 – Main lung lesion. Axial contrast-enhanced CT image, arterial-phase, shows predominant lung lesion localized to the middle lobe, about 3 cm in size) that appears mostly hypodense with numerous contextual dilated vessels (arrow).

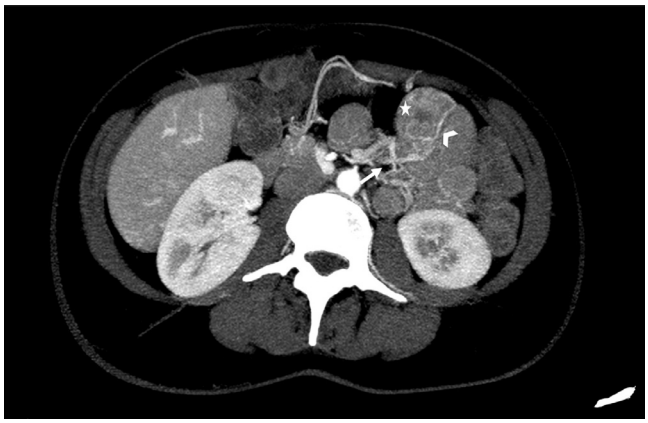

Fig. 3 – Jejunal wall lesion with tumor induced neoplastic angiodysplasia. Axial contrast-enhanced CT image, arterial-phase, MIP reconstruction, shows congestion and inhomogeneous mural enhancement of jejunal wall (star), with coexistence of intramural swollen vessels (arrowhead) and associate early impregnation of mesenteric drainage veins (harrow).

Fig. 4 – Hepatic metastasis' necrotic-hemorrhagic degeneration. Axial contrast-enhanced CT image, venous-phase, shows a large subcapsular hematoma in the right liver (stars), with evident of liver metastases coalescence and necrotic-hemorrhagic aspects changes, with conspicuous central necrosis (arrow) as well as signs of bleeding (arrowhead).

Then the first cycle of chemotherapy was administered. Unfortunately, on the fourth day of therapy, she developed abdominal pain and distension with a rapidly declining hematocrit suggesting a new active bleeding, confirmed by CE-CT examination. Imaging showed a large subcapsular hematoma in the right liver, with evident necrotic-hemorrhagic aspects. Moreover, liver metastases tended to coalesce and showed a more conspicuous central necrosis as well as signs of bleeding (Fig. 4). Hemoperitoneum was also present. Interestingly, the most peculiar imaging finding was the appearance of bilaterally enlarged ovaries with 2 multiloculated cystic masses, with thin septa and fluid attenuation values (range 2-15 HU). Furthermore, few small solid intracystic nodules were evident. These multicystic masses measured 9 × 6 × 11 cm on the right side and 11 × 9 × 15 cm on the left side, respectively (Fig. 5). Uterus had a normal size and morphology. Ascites was also observed, mainly in the pelvic cavity. The differential diagnosis of ovarian neoplastic localization was taken into consideration, but the radiological features were more consistent with a functional pathology. Thus, basing on the clinical, laboratory and radiological findings, a provisional diagnosis of OHSS induced by high levels of b-hCG was made. The patient underwent a new emergency surgery with right subtotal hepatectomy, excision of the larger lesions of the left hemi-liver and bilateral adnexectomy. Histopathological examination of the ovarian sample confirmed our hypothesis, revealing multiple luteinized follicular macrocysts some of which had serum-blood like content, while the solid intracystic nodules seen on CT were found to be hemorrhagic corpora lutea. However, after a gradual stabilization of the clinical condition, the patient resumed chemotherapy. Follow-up CT scans showed partial and progressive response to treatment with the reduction of liver and lung metastases.

Fig. 5 – Adnexal multiloculated and multilobulated cystic masses. Axial contrast-enhanced CT image, venous-phase, shows bilaterally enlarged ovaries with 2 multiloculated and multilobulated cystic masses, with thin septa and fluid attenuation values (range 2-15 HU) with few small solid intracystic nodules (arrow).

Discussion

Gestational choriocarcinoma is the most aggressive form of gestational trophoblastic neoplasia due to its local invasiveness and marked tendency to metastasize, but it is generally responsive to chemotherapy. Most of the time occurs in the uterus but in some patients it can manifest as disseminated disease, without a clearly detectable uterine mass [4–6].

According to some hypothesis of literature, these forms may represent metastases from undetected trophoblastic disease, which might undergo a spontaneous regression merely leaving scarring of the uterus. It is also possible that choriocarcinoma develops from trophoblastic emboli in other organs, related to a gestational event after a long period of latency [10]. Post-molar forms are usually diagnosed early thanks to b-hCG surveillance, mostly in asymptomatic patients. Non-molar choriocarcinoma is more insidious and may present with abnormal uterine bleeding (with a variable latency from months to years after delivery) [11] or have an acute onset with symptoms related to distant metastases, as in our patient. Imaging plays a fundamental role in the diagnosis and staging of choriocarcinoma and can rapidly assess its main complications. Pelvic US is the modality of choice for initial evaluation, allowing to identify or rule out a pelvic mass, while MRI provides a reliable assessment of the spread of disease in the pelvis. CE-CT can detect extra-pelvic localizations and provides disease staging. Brain MR imaging is the gold standard for the characterization of central nervous system metastases [12]. However, the imaging findings are not pathognomonic and must be supported by the patient's clinical history and high b-hCG levels. In our patient, the diagnosis of metastatic gestational choriocarcinoma was supported by the previous pregnancy history, the high b-hCG level and CT findings. It was subsequently confirmed by histological examination and favorable response to chemotherapy. The peculiarity of our case was the absence of demonstrable uterine localization in presence of jejunal, liver and pulmonary lesions. Choriocarcinoma is characterized by marked neoangiogenesis, early and extensive vascular invasion resulting in high tendency to metastasize through the hematogenous route even when the primary tumor is quite small or not detectable. Metastasis commonly spreads to the lung (80%), followed by vagina (30%), brain (10%), and liver (10%) [13]. It may also metastasize to kidney, gastrointestinal tract, skin, or fetus but isolated metastasis to other sites is rare in the absence of lung metastasis [12]. It is frequent to observe hypervascular metastases with imaging features similar to the primary lesion, such as heterogeneous necrotic areas due to rapid growth and hemorrhagic changes as a consequence of high vascularity [12]. Lung metastases are typically multiple well-defined, rounded, soft-tissue attenuation pulmonary nodules, although some patients may present with a single nodule. On CT a common pattern is a peripheral ground-glass attenuation surrounding the nodules (halo sign), which results from peritumoral hemorrhage [14]. In some cases, cavitary and bulla-forming pulmonary metastases may occur, which can result in pneumothorax [15]. Brain metastases are usually multiple, located at grey-white matter junctions, with hemorrhage and surrounding edema. On unenhanced CT we can have hyperdense lesions due to bleeding with variable signal intensity on MRI depending on the age of the intralesional hemorrhage. Owing to their hypervascular nature, the lesions have avid contrast enhancement in post-contrast imaging [16]. Liver metastases occur later in the course of disease and typically seen as multiple hypervascular lesions on both CT and MRI, showing avid contrast enhancement in the arterial phase and sometimes hemorrhagic transformation with a central hypodense necrotic component. They are indistinguishable from other hypervascular liver lesions and should never be biopsied due to high hemorrhage risk [17-18]. However, the imaging findings are non-specific and require clinical-laboratory support. The differential diagnosis should include hypervascular metastases from renal cell carcinoma, thyroid carcinoma, angiosarcoma, or hemangioendothelioma [12]. A life-threatening complication of the widespread disease is the "choriocarcinoma syndrome" consisting in extensive hemorrhage in either primary tumor and/or its metastases, as occurred in our patient (Fig. 6) [19]. Hemorrhage can occur both in patients with progressive advanced disease and immediately after the start of chemotherapy. The hemorrhagic syndrome reflects the tumoral high vascularity and the innate capacity of trophoblastic cells to invade and erode vessel wall [20,21]. Furthermore, neoplastic angiogenesis causes fragility of the tumor vessels and arteriovenous shunts. Metastases can produce pseudoaneurysms or arteriovenous fistulas prone to bleeding [22]. Clinical manifestations range from progressive anemization to hemodynamic instability and hemorrhagic shock. Multiphasic CT is the diagnostic modality of choice in case of suspected hemorrhagic complications due to its rapid availability and excellent spatial and contrast resolution for depiction of small vessels which, together with the possibility of image post-processing options, can allow getting important information about the cause and site of bleeding. In the gastrointestinal tract, hemorrhage can manifest in a wide spectrum of gravity, from occult bleeding, multiple episodes of melena up to massive bleeding [23,24]. As in our patient, intestinal lesions can have an insidious appearance on imaging CT, with poor wall thickening without a well-defined lesion, no perivisceral tissue reaction or lymphadenopathy. The lesions may have an angiodysplasia-like appearance. We observed inhomogeneous focal areas of increased enhancement in bowel walls with swollen and hypertrophic intramural vessels, brightest on enteric phase, can be observed. The earlier filling of enlarged antimesenteric veins is a typical sign of arteriovenous shunting, better visualized using Maximum Intensity Projection (MIP) and Multi-Planar Reconstruction (MPR) post-processing (Fig.6) (Fig. 7). These findings can simulate angiodysplasia. CT angiography can demonstrate leak of contrast agent into the intestinal lumen. However, as in our case, CE-CT may show low sensitivity in demonstrating intestinal bleeding, possibly due to intermittent or low intensity bleeding below its detection threshold [25]. Thus, in these cases, further diagnostic investigation like Technetium 99m-labeled red blood cell scintigraphy can be necessary [26]. In the liver, hemorrhagic metastases can show areas of higher attenuation on pre-contrast scan as signs of recent bleeding and/or active extravasation in post-contrast phases. The rapid growth of the neoplastic tissue can lead to extensive necrotic-colliquative changes with coexisting hemorrhage. Rupture of hemorrhagic liver metastases can lead to subcapsular hematomas up to hemoperitoneum [27]. Lung lesions can also be hemorrhagic; typical imaging findings are perilesional ground glass attenuation (halo sign) up to extensive patchy ground-glass opacities consistent with diffuse alveolar hemorrhage. Hemothorax has also been reported [28]. Cerebral hemorrhage can be caused by bleeding within the tumor mass or by the development of neoplastic aneurysms whose rupture leads to intraparenchymal or subarachnoid hemorrhage [29]. Another peculiar aspect of

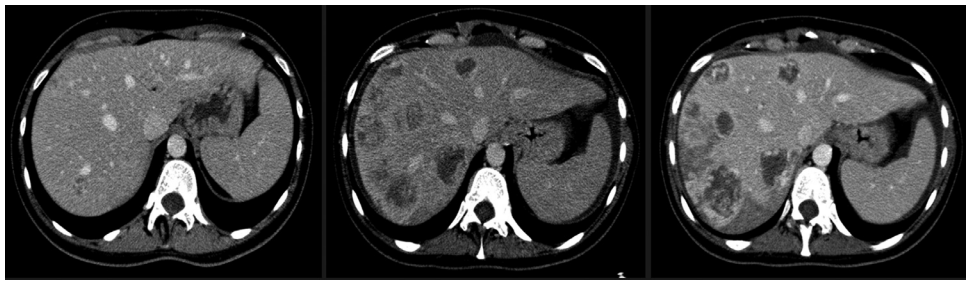

Fig. 6 – Choriocarcinoma syndrome development. Axial contrast-enhanced CT image, venous-phase, form subsequent CT controls in about 2 weeks, shows (from left to right) increasing and necrotic-hemorrhagic aspects changes of hepatic metastasis with development of bleeding and large subcapsular hematoma in the right liver induced by tumor hypervascular nature, configuring a framework of choriocarcinoma syndrome.

Fig. 7 – Neoplastic angiodysplasia MPR and MIP reconstruction. Axial (on the left) and sagittal (on the right) contrast-enhanced CT images, arterial-phase, MPR and MIP reconstruction, show inhomogeneous focal areas of increased enhancement in bowel wall (arrowhead) with swollen and hypertrophic intramural vessels, with earlier filling of enlarged antimesenteric veins (arrow), typical sign of indicating arteriovenous shunting, better visualized due to using Maximum Intensity Projection (MIP) and Multi-Planar Reconstruction (MPR) post-processing. These findings are typical of neoplastic angiodysplasia.

our case is the ovarian hyperfunction induced by the tumor. At first imaging evaluation, the ovaries were completely normal. Subsequent CT showed enlarged ovaries with multicystic masses due to progressive hormonal stimulation (Fig. 8). It was a rare case of spontaneous OHSS associated with an extragonadal b-hCG secreting tumor. This syndrome is a rare iatrogenic complication of assisted reproduction techniques due to ovarian stimulation by exogenous hormones [30]. However, it may exceptionally be spontaneous in nature, caused by the overproduction of endogenous stimulating hormones, without any external stimulation. In literature, non- iatrogenic OHSS has been described in pregnancy (especially multiple), gestational trophoblastic disease, b-hCG - secreting tumors, FSH/LH-secreting pituitary adenomas, and high levels of TSH in hypothyroidism [31,32]. The OHSS is characterized by the combination of massive ovarian multicystic masses and potential complication due to increased vascular permeability induced by high hormonal level [33]. This syndrome's pathogenesis is still poorly understood. It has been suggested that abnormally high levels of b-hCG (or other glycoprotein hormones like TSH, LH, and FSH) are responsible for the promiscuous hyperstimulation of FSH receptors expressed in developing ovarian follicles [34].

According to other hypothesis, the follicular growth is caused by a variant of b-hCG with greater biological activity for wild- type FSH receptor, while a mutated FSH receptor with abnormal sensitivity to b-hCG has been implicated in OHSS that occurs in normal pregnancy [35]. In all cases, however, the hormonal stimulation is responsible for cystic ovarian enlargement due to theca-lutein cysts caused by luteinization and hypertrophy of the theca interna cell layer. The multiple corpora lutea are responsible for the massive production of vasoactive substances implicated with increased vascular permeability. The presentation can range from mild OHSS, characterized by asymptomatic ovarian enlargement, up to severe forms with life-threatening complications due to increased vascular permeability responsible for fluid-shift into third space compartments [36]. OHSS's manifestations can be abdominal pain, ascites, pleura and/or pericardial effusion up to electrolyte disorders, hemoconcentration, hypovolemia and oliguria; coagulative disorders have also been described. However, severe form is less common [37]. Imaging findings are superimposable in US, CT, and MRI: symmetrical enlargement of the ovaries, often measuring >12 cm in size, is observed with multiple thin-walled cysts of varying sizes. In some cases, they have a "spoke-wheel" appearance due to the central position

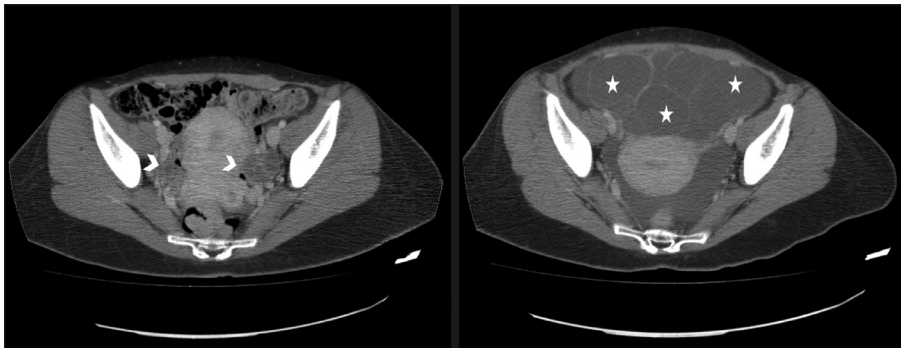

Fig. 8 – Development of b-hCG induced ovarian hyperstimulation syndrome. Axial contrast-enhanced CT images, venous-phase, on the left first imaging evaluation with normal ovaries (arrowheads). On the right subsequent check shows enlarged ovaries with multicystic masses (stars) due to progressive hormonal stimulation. a rare case of spontaneous OHSS associated with extragonadal b-hCG -secreting tumor.

of ovarian stroma surrounded by numerous large peripheral cysts, which may be hemorrhagic [38]. No significant vascularization of solid intracystic components is evident, except for any corpora lutea that usually present an enhanced rim. Ascites, pleural and/or pericardial effusion can be present [39]. Clinical suspicion of OHSS in a patient with diagnosis of choriocarcinoma is difficult due to its rare incidence and overlapping complications deriving from hemorrhagic syndrome. In our case, it was an incidental discovery on CT performed to look for ongoing bleeding. It can't be emphasized enough the importance of the imaging findings together with laboratory data which allowed us to hypothesize OHSS, excluding ovarian neoplastic localization.

Disclaimer

We confirm that this work is original and has not been published elsewhere nor is it currently under consideration for publication elsewhere.

Publication is approved by all authors and by the responsible authorities where the work was carried out.

Each author have participated sufficiently in any submission to take public responsibility for its content.

Patient consent

Informed consent was obtained by the patient for publication of this case.

REFERENCES

[1] Rao KV, Konar S, Gangadharan J, Vikas V, Sampath S. A pure non-gestational ovarian choriocarcinoma with delayed solitary brain metastases: case report and review of the literature. J Neurosci Rural Pract 2015;6(4):578–81. doi:10.4103/0976-3147.169869.

[2] Ghaemmaghami F, Karimi Zarchi, M. Early onset of metastatic gestational trophoblastic disease after full-term pregnancy. Int J Biomed Sci 2008;4(1):74–7.

[3] Hou MM, Xu L, Qie MR. Postmolar choriocarcinoma after an interval of 7 years: case report and literature review. Gynecol Minim Invasive Ther 2017;6(4):207–10. doi:10.1016/j.gmit.2017.07.002.

[4] Li HM, Hou WC, Lai YJ, Kao CC, Chao TK, Yu MH, et al. Gestational choriocarcinoma with renal and pulmonary metastases lacking a primary uterine origin. Taiwan J Obstet Gynecol 2016;55(6):881–5. doi:10.1016/j.tjog.2015.08.028.

[5] Kanehira K, Starostik P, Kasznica J, Khoury T. Primary intraplacental gestational choriocarcinoma: histologic and genetic analyses. Int J Gynecol Pathol 2013;32(1):71–5. doi:10.1097/PGP.0b013e3182566552.

[6] Soper JT, Mutch DG, Schink JCAmerican College of Obstetricians and Gynecologists. Diagnosis and treatment of gestational trophoblastic disease: ACOG Practice Bulletin No. 53. Gynecol Oncol 2004;93(3):575–85. doi:10.1016/j.ygyno.2004.05.013.

[7] Waseda Y, Komai Y, Yano A, Fujii Y, Noguchi N, Kihara K. Pathological complete response and two-year disease-free survival in a primary gastric choriocarcinoma patient with advanced liver metastases treated with germ cell tumor-based chemotherapy: a case report. Jpn J Clin Oncol 2012;42(12):1197–201. doi:10.1093/jjco/hys164.

[8] Liu Y, Yang J, Ren T, Zhao J, Feng F, Wan X, et al. The encouraging prognosis of nongestational ovarian choriocarcinoma with lung metastases. J Reprod Med 2014;59(5-6):221–6.

[9] Ramachandran BS, Murugesan M, Ali M, Padmanabhan P. Primary pancreatic choriocarcinoma presenting as pancreatitis. JOP 2012;13(2):217–18.

[10] Wu PS. Primary choriocarcinoma of the lung: a case report and literature review. Int J Clin Exp Pathol 2020;13(9):2352–2355.

[11] Tidy JA, Rustin GJ, Newlands ES, Foskett M, Fuller S, Short D, et al. Presentation and management of choriocarcinoma after nonmolar pregnancy. Br J Obstet Gynaecol 1995;102(9):715–19. doi:10.1111/j.1471-0528.1995.tb11429.x.

[12] Shaaban AM, Rezvani M, Haroun RR, Kennedy AM, Elsayes KM, Olpin JD, et al. Gestational trophoblastic disease: clinical and imaging features. Radiographics 2017;37(2):681–700. doi:10.1148/rg.2017160140.

[13] Milenković V, Lazović B, Mačvanski M, Jeremić K, Hrgović Z. Clinical outcome of a FIGO stage IV gestational

choriocarcinoma. Case Rep Oncol 2013;6(3):504–7. doi:10.1159/000353626.
[14] Seo JB, Im JG, Goo JM, Chung MJ, Kim MY. Atypical pulmonary metastases: spectrum of radiologic findings. Radiographics 2001;21(2):403–17. doi:10.1148/radiographics.21.2.g01mr17403.
[15] Hyun K, Jeon HW, Kim KS, Choi KB, Park JK, Park HJ, et al. Bullae-forming pulmonary metastasis from choriocarcinoma presenting as pneumothorax. Korean J Thorac Cardiovasc Surg 2015;48(6):435–8. doi:10.5090/kjtcs.2015.48.6.435.
[16] Athanassiou A, Begent RH, Newlands ES, Parker D, Rustin GJ, Bagshawe KD. Central nervous system metastases of choriocarcinoma. 23 years' experience at Charing Cross Hospital. Cancer 1983;52(9):1728–35 10.1002/1097-0142(19831101)52:9<1728::aid-cncr2820520929>3.0.co;2-u.
[17] Kang YJ, Oh JH, Yoon Y, Kim EJ, Kim DY, Kang HS. Hepatic metastasis from choriocarcinoma: angiographic findings in two cases. Korean J Radiol. 2002;3(4):260–3. doi:10.3348/kjr.2002.3.4.260.
[18] Gulati A, Vyas S, Lal A, Harsha TS, Gupta V, Nijhawan R, et al. Spontaneous rupture of hepatic metastasis from choriocarcinoma: a review of imaging and management. Ann Hepatol 2009;8(4):384–7.
[19] Medina A, Ramos M, Amenedo M, París L. Choriocarcinoma syndrome. Arch Esp Urol 2014;67(8):711–14.
[20] Rejlekova K, Cursano MC, De Giorgi U, Mego M. Severe complications in testicular germ cell tumors: the choriocarcinoma syndrome. Front Endocrinol (Lausanne) 2019;10:218. doi:10.3389/fendo.2019.00218.
[21] Arana S, Fielli M, González A, Segovia J, Villaverde M. Choriocarcinoma syndrome in a 24-year-old male. JRSM Short Rep 2012;3(6):44. doi:10.1258/shorts.2012.012004.
[22] Kalafut M, Vinuela F, Saver JL, Martin N, Vespa P, Verity MA. Multiple cerebral pseudoaneurysms and hemorrhages: the expanding spectrum of metastatic cerebral choriocarcinoma. J Neuroimaging 1998;8(1):44–7. doi:10.1111/jon19988144.
[23] Heil R, Tran T, Stawick L, Herschman B. Metastatic choriocarcinoma of the small intestine presenting as refractory anemia and melena. ACG Case Rep J 2015;2(3):131–2. doi:10.14309/crj.2015.30.
[24] Yoon J, Hu S, Farrell J, Shah KK, Chintanaboina JK. An exceptionally rare cause of refractory gastrointestinal bleed: choriocarcinoma syndrome. Cureus 2021;13(4):e14599. doi:10.7759/cureus.14599.
[25] García-Blázquez V, Vicente-Bártulos A, Olavarria-Delgado A, Plana MN, van der Winden D, Zamora J, et al. Accuracy of CT angiography in the diagnosis of acute gastrointestinal bleeding: systematic review and meta-analysis. Eur Radiol 2013;23(5):1181–90. doi:10.1007/s00330-012-2721-x.
[26] Emslie JT, Zarnegar K, Siegel ME, Beart RW Jr. Technetium-99m-labeled red blood cell scans in the investigation of gastrointestinal bleeding. Dis Colon Rectum 1996;39(7):750–4. doi:10.1007/BF02054439.
[27] Gulati A, Vyas S, Lal A, Harsha TS, Gupta V, Nijhawan R, et al. Spontaneous rupture of hepatic metastasis from choriocarcinoma: a review of imaging and management. Ann Hepatol 2009;8(4):384–7.
[28] Pearce H, Edwards DC, Levy JA, McGreen BH, Mackovick L, Brennan M, et al. Acute pulmonary hemorrhage associated with metastatic testicular choriocarcinoma in a 46-year-old incarcerated male. Urol Ann 2019;11(1):109–12. doi:10.4103/UA.UA_51_18.
[29] Huang CY, Chen CA, Hsieh CY, Cheng WF. Intracerebral hemorrhage as initial presentation of gestational choriocarcinoma: a case report and literature review. Int J Gynecol Cancer 2007;17(5):1166–71. doi:10.1111/j.1525-1438.2007.00934.x.
[30] Delvigne A, Rozenberg S. Epidemiology and prevention of ovarian hyperstimulation syndrome (OHSS): a review. Hum Reprod Update 2002;8(6):559–77. doi:10.1093/humupd/8.6.559.
[31] Agrawal NR, Gupta G, Verma K, Varyani N. Spontaneous ovarian hyperstimulation syndrome in a triplet pregnancy. Case Rep Crit Care 2012;2012:189705. doi:10.1155/2012/189705.
[32] Ilanchezhian S, Mohan SV, Ramachandran R, Babu SR. Spontaneous ovarian hyperstimulation syndrome with primary hypothyroidism: imaging a rare entity. Radiol Case Rep 2015;10(1):1050. doi:10.2484/rcr.v10i1.1050.
[33] Mittal K, Koticha R, Dey AK, Anandpara K, Agrawal R, Sarvothaman MP, et al. Radiological illustration of spontaneous ovarian hyperstimulation syndrome. Pol J Radiol 2015;80:217–27. doi:10.12659/PJR.893536.
[34] Delbaere A, Smits G, De Leener A, Costagliola S, Vassart G. Understanding ovarian hyperstimulation syndrome. Endocrine 2005;26(3):285–90. doi:10.1385/ENDO:26:3:285.
[35] Smits G, Campillo M, Govaerts C, Janssens V, Richter C, Vassart G, et al. Glycoprotein hormone receptors: determinants in leucine-rich repeats responsible for ligand specificity. EMBO J 2003;22(11):2692–703. doi:10.1093/emboj/cdg260.
[36] Golan A, Ron-el R, Herman A, Soffer Y, Weinraub Z, Caspi E. Ovarian hyperstimulation syndrome: an update review. Obstet Gynecol Surv 1989;44(6):430–40. doi:10.1097/00006254-198906000-00004.
[37] Delvigne A, Rozenberg S. Review of clinical course and treatment of ovarian hyperstimulation syndrome (OHSS). Hum Reprod Update 2003;9(1):77–96. doi:10.1093/humupd/dmg005.
[38] Jung BG, Kim H. Severe spontaneous ovarian hyperstimulation syndrome with MR findings. J Comput Assist Tomogr 2001;25(2):215–17. doi:10.1097/00004728-200103000-00009.
[39] Nwafor NN, Nyoyoko NP. Spontaneous ovarian hyperstimulation syndrome: a report of two cases from different pathogenesis. Niger Med J 2020;61(5):269–72. doi:10.4103/nmj.NMJ_183_20.